AN OBSERVATIONAL DETECTION OF THE BRIDGE EFFECT OF VOID FILAMENTS

Junsup Shim[1], Jounghun Lee[1], Fiona Hoyle[2]

ABSTRACT

The bridge effect of void filaments is a phrase coined by Park & Lee (2009b) to explain the correlations found in a numerical experiment between the luminosity of the void galaxies and the degree of the straightness of their host filaments. Their numerical finding implies that a straight void filament provides a narrow channel for the efficient transportation of gas and matter particles from the surroundings into the void galaxies. Analyzing the Sloan void catalog constructed by Pan et al. (2012), we identify the filamentary structures in void regions and determine the specific size of each void filament as a measure of its straightness. To avoid possible spurious signals caused by the Malmquist bias, we consider only those void filaments whose redshifts are in the range of $0 \leq z \leq 0.02$ and find a clear tendency that the void galaxies located in the more straight filaments are on average more luminous, which is in qualitative agreement with the numerical prediction. It is also shown that the strength of correlation increases with the number of the member galaxies of the void filaments, which can be physically understood on the grounds that the more stretched filaments can connect the dense surroundings even to the galaxies located deep in the central parts of the voids. This observational evidence may provide a key clue to the puzzling issue of why the void galaxies have higher specific star formation rates and bluer colors than their wall counterparts.

Subject headings: cosmology:theory — large-scale structure of universe

[1]Astronomy Program, Department of Physics and Astronomy, FPRD, Seoul National University, Seoul 151-747, Korea

jsshim@astro.snu.ac.kr, jounghun@astro.snu.ac.kr

[2]Pontifica Universidad Catolica de Ecuador, 12 de Octubre 1076 y Roca, Quito, Ecuador

1. INTRODUCTION

Despite its extreme low-density, a void exhibits a dilute miniature of the cosmic web that interconnects the void galaxies (e.g., Sahni et al. 1994; Gottlöber et al. 2003; Kreckel et al. 2011; Aragon-Calvo & Szalay 2013; Alpaslan et al. 2014). The anisotropic spatial correlation of the tidal shear field is believed to be mainly responsible for the formation of the mini-web in a void just as it is for the cosmic web in the whole universe (van de Weygaert & van Kampen 1993; Bond et al. 1996). As the tidal shear field develops nonlinear correlations during the evolutionary process, the mini-web in a void region should become more and more filamentary.

An intriguing issue is what effect the filamentary mini-web has on the evolution of the void galaxies and how strong it is. This can be addressed by looking for correlations between the intrinsic properties of the void galaxies and the characteristics of the void filaments. In fact, the voids should be an optimal ground for the investigation of the effect of the filamentary web on the galaxy evolution (e.g., see Kreckel et al. 2011). First of all, since the void filaments are much less intricate than their wall counterparts, it is less difficult to identify and characterize them. Furthermore, since the densities of the voids are all constrained to extremely low values, the effect of the environmental density on the properties of the void galaxies can be controlled and thus it should be easier to single out the dependence of the galaxy properties on the filamentary web for the case of the void galaxies.

The mini-filaments that pass through a void are expected to bridge the void galaxies with the surrounding denser regions. Hence, the gas and dark matter from the surroundings can be transported into the void regions along the mini-filaments, which would enhance the growth of the void galaxies (Park & Lee 2009b; Kreckel et al. 2011). The recent observation of Beygu et al. (2013) which reported a detection of real-time star-forming activities in the void galaxies embedded in the filamentary channels full of HI cold gases is in line with this picture that the void galaxies can rapidly grow through the filamentary connection with the surroundings.

The bridge effect of void filaments was first noted and quantitatively investigated in the numerical work of Park & Lee (2009b) using the Millennium Run semi-analytic galaxy catalog (Springel et al. 2005). What they found was that the intrinsic properties of the void galaxies such as the total mass, luminosity and blackhole mass are strongly correlated with the degree of the straightness of the host filaments. Park & Lee (2009b) suggested that the presence of this correlation should be attributed to the dependence of the efficacy of gas transportation on the geometrical shapes of the void filaments: the more straight void filaments should more efficiently carry gas and matter onto the void galaxies. Here, our goal is to detect the bridge effect of the void filament from observational data.

The upcoming sections are outlined as follows. In Section 2 we describe how the void filaments are identified from the Sloan void catalog and how the degrees of their straightness are measured. In Section 3 we report an observational detection of the correlation signals between the luminosities of the void galaxies and the degrees of the straightness of their host filaments. In Section 4 we summarise the results and discuss what clues we can obtain to the formation and evolution of the void galaxies from this observational detection as well as what future works would improve the current analysis. Throughout this paper, we assume a flat ΛCDM universe where the cosmological constant Λ and cold dark matter (CDM) dominate at the present epoch whose initial conditions are described by $\Omega_m = 0.27,\ \Omega_\Lambda = 0.73,(h = 0.7, \sigma_8 = 0.8)$, to be consistent with Pan et al. (2012).

2. IDENTIFYING THE MINI-FILAMENTS FROM THE SLOAN VOIDS

Since there is no unique way to define both the filaments and the voids, it is first necessary to decide on which algorithm to use for the identification of both. In the current analysis, to be consistent with Park & Lee (2009b), we choose the filament-finding and the void-finding algorithms developed by Colberg (2007) and Hoyle & Vogeley (2002, hereafter HV02), respectively. The former is based on the minimal spanning tree (MST) technique to find the networking pattern (i.e., MST) in the spatial distributions of the point sources and identify the filamentary structures as the most conspicuous cylindrical structures in the interconnected MSTs (Barrow et al. 1985; Colberg 2007).

In the HV02 algorithm, a void is identified as an underdense region containing only field but no wall galaxies. The distance to the fourth nearest galaxy was used as a criterion for the classification of a galaxy: For the wall (field) galaxy, $d \le d_{\rm th}$ ($d > d_{\rm th}$) where $d_{\rm th}$ is a given threshold distance whose value depends on the parent sample of the galaxies (El-Ad & Piran 1997). The boundary of a void is approximated by the continuous surfaces of the superimposed spheres that fit the underdense region (El-Ad & Piran 1997; Hoyle & Vogeley 2002).

Pan et al. (2012) constructed a catalog of the local voids by applying the HV02 algorithm to the seventh Data Release of the Sloan Digital Sky Survey (SDSS DR7)(Abazajian et al. 2009). The void catalog contains a total of 1055 giant voids in the redshift range of $0 \le z \le 0.107$. It is basically a magnitude-limited sample of the void galaxies for each of which information on redshift, equatorial coordinates and the r-band magnitude is all available. The effective radii ($R_{\rm eff}$) and the numbers of the member galaxies ($N_{\rm g}$) of the voids were found to be in the ranges of $9.85 \le R_{\rm eff}/(h^{-1}{\rm Mpc}) \le 33.92$ and $2 \le N_{\rm g} \le 2984$, respectively (Pan et al. 2012).

As Park & Lee (2009b) did, we exclude those voids which have less than thirty member galaxies from the void catalog of Pan et al. (2012) on the grounds that the filamentary structures are hard to find from those voids. A sample of 831 giant local voids is constructed to which we apply the MST-based filament finding algorithm as follows. For each void in the sample, the member galaxies are regarded as points. The link between a randomly chosen point and its nearest point forms an initial MST, which grows and become updated as the other points in the same void are sequentially added to it in an decreasing order of the separation distances via an iterative search for the nearest points.

A full MST comes out from each void if all of the points become connected. The void filaments are obtained by reducing down a full MST, which requires us to specify two parameters: the pruning level p and the separation threshold d_c. After the minor branches consisting of less than p points are all pruned away, the remaining part of the MST is separated into several mini-filaments by disjoining the galaxies whose separation distances are larger than a given threshold d_c (Colberg 2007). For the detailed description of the MST-based filament identification procedures applied to the void regions, see Park & Lee (2009a) and Park & Lee (2009b).

As done in Colberg (2007) and Park & Lee (2009b), the best pruning level p is determined as the value at which the size distribution of the void filaments becomes stabilized in the large size section, where the size S of a filament is defined as the spatial extent of the three dimensional positions of its member galaxies. The size distribution of the void filaments, $dN/d\log S$, is calculated as the number of the void filaments whose sizes S belong to the differential interval $[\log S, \log S + d\log S]$ (Park & Lee 2009a).

Varying the pruning level p from 2 to 7, we repeatedly apply the MST-based filament finder to the 831 giant voids and determine $dN/d\log S$. Figure 1 plots the size distributions of the void filaments from our void sample, $dN/d\log S$, for six different cases of the pruning level p. For the case of $p \leq 4$, the functional form of $dN/d\log S$ fluctuates with the change of p in the large size section ($S \geq 10\,h^{-1}$Mpc). However, note that it becomes stabilized against the change of p if p reaches and exceeds 5, which leads us to determine the best pruning level to be $p = 5$. It is interesting to recall that in the numerical experiment of Park & Lee (2009b) the size distribution of the void filaments from the Millennium semi-analytic galaxy catalog was shown to become stabilized at the same pruning level $p = 5$.

Since the best value of p depends on the number of the sample galaxies, we investigate how the best value of p changes if the minimum number of the void galaxies, say $N_{\rm g,min}$, differs from the threshold value of 30 adopted by Park & Lee (2009b). Varying the value of $N_{\rm g,min}$ from 20 to 50, we repeat the whole process to evaluate $dN/d\log S$, which is shown in Figure 2. Although the number density of the void filaments with large sizes ($S \geq 5\,h^{-1}$Mpc)

decreases substantially as the value of $N_{\rm g,min}$ increases, it is found that the four different cases of $N_{\rm g,min}$ yield the same pruning level $p = 5$. Furthermore, the correlation strength between the luminosity and the straightness of the void filaments quantified by the Pearson product moment correlation coefficient r turns out to be robust against the change of $N_{\rm g,min}$ (see section 3). Throughout this paper, we set $N_{\rm g,min}$ at 30 to be consistent with Park & Lee (2009b).

To determine the value of d_c, Park & Lee (2009b) sought for the value which maximizes the number of the void filaments consisting of four and more member galaxies. They excluded the filaments with less than four member galaxies since those filaments should always have high degree of straightness. Park & Lee (2009b) noted that the number of the void filaments with four and more member galaxies varies strongly with d_c and reached the highest value when d_c is equal to $\bar{d} + \sigma_d$ where $\bar{d}$ and σ_d are the mean and the standard deviation of the separation distances of the member galaxies belonging to the unpruned MSTs, respectively. Following Park & Lee (2009b), we calculate the values of $\bar{d}$ and σ from the unpruned MSTs of the void galaxies found in the Sloan void catalog of Pan et al. (2012), we determine the critical separation distance d_c as $d + \sigma_d$.

Among a total of 3172 void filaments found in the redshift range of $0 \le z \le 0.107$ from the Sloan void catalog of Pan et al. (2012), the richest one turns out to have 38 nodes where the node is a jargon of the MST algorithm referring to a member galaxy of a filament (Colberg 2007). Figure 3 shows the number of the void filaments $N_{\rm fil}$ as a function of the number of their nodes, $N_{\rm node}$, in our sample. For the right-most bin, we plot the accumulated numbers of the void filaments which have 13 or more nodes. As can be seen, the number of the void filaments $N_{\rm fil}$ decreases sharply with the number of the nodes $N_{\rm node}$, indicating that the filaments are relatively short in the voids compared with the wall counterparts.

3. CORRELATIONS BETWEEN THE GALAXY LUMINOSITY AND THE SPECIFIC SIZES OF VOID FILAMENTS

In the original work of Park & Lee (2009b) based on a N-body simulation, the linearity, $R_{\rm L}$, of each filament, defined as the ratio of its end-to-end separation to its total length was used as an indicator of the straightness where the total length of a void filament was defined as the sum of the separation distances between the adjacent nodes (see also Colberg 2007; Park & Lee 2009a). However, in our current work dealing with the void filaments from real observations identified in redshift space, the linearity $R_{\rm L}$ may not be a good indicator of the degree of the straightness of a void filament since the total length of a void filament that enters in the definition of $R_{\rm L}$ depends sensitively on how accurately the positions of the void

galaxies are measured.

The systematic errors associated with the redshift-space measurement of $R_{\rm L}$ may severely contaminate the measurement of the correlations between the luminosity of the void galaxies and the degree of the straightness of the hosting void filaments. Therefore, instead of $R_{\rm L}$, we use the specific size of each void filament, $\tilde{S}$, defined as the size per node as an indicator of the straightness. The concept of the specific size of a filamentary structure was first introduced by Shim & Lee (2013) who showed that the filamentary structures having larger specific sizes tend to have more straight shapes (see Figure 6 in Shim & Lee 2013).

For each void filament in our sample, we also determine the mean absolute value , $|\bar{M}_r|$, of the absolute r-band magnitudes of the member galaxies. Since the absolute magnitude M_r of a galaxy has a negative value and what matters in the current analysis is not the sign but the magnitude of M_r, we take the absolute value of $|\bar{M}_r|$ to investigate the correlation with the specific size of the hosting void filament. From there on, $|\bar{M}_r|$ denotes the mean absolute value of M_r averaged over the member galaxies of each void filament in the sample.

Figure 4 plots how the void filaments in our sample are scattered in the plane spanned by $|\bar{M}_r|$ and $\tilde{S}$, showing an obvious trend that the averaged luminosity of the void galaxies increases with the degree of the straightness of their host filament. Before interpreting this trend as an observational evidence for the bridge effect of the void filaments, it should be critical to examine the possibility that the trend might be just a consequence of the Malmquist bias (Malmquist 1936). Given that the Sloan void catalog of Pan et al. (2012) is a magnitude-limited sample, the high-z void filaments must be biased being composed only of very luminous galaxies. Since the mean separation distance obtained from a sample including only the very luminous galaxies should be larger than than from a sample including the dim galaxies, the separation threshold d_c that is used as a criterion to separate each MST into filaments (see Section 2) tends to have a larger value for the case of the high-z voids. Therefore, the void filaments identified at high-redshifts via the MST algorithm are likely to have more extended spatial sizes per node, which would in turn create a spurious signal of correlation between $|\bar{M}_r|$ and $\tilde{S}$.

There are two different ways to remove the Malmquist bias. The first way is to construct a volume-limited sample of the void galaxies up to $z = 0.107$ by excluding the dim galaxies below the corresponding threshold magnitude limit. The second one is to consider only the nearby void filaments located at the lowest redshifts. We choose the second direction for the following reason. As mentioned in Park & Lee (2009b), the bridge effect is believed to be related to the effect of the anisotropic tidal shear field on the evolution of the void galaxies (see also Section 4 for a full discussion). Thus, to detect a genuine signal of the bridge effect, it is important to identify the void filaments whose straightness can reflect

well the anisotropic nature of the tidal shear field. If the void filaments are found in the volume-limited sample of the luminous galaxies above the corresponding magnitude limit, it is likely that the degree of their straightness fails to represent the degree of anisotropy of the tidal shear field because the luminous galaxies are the biased tracers of the matter density field. As the luminous galaxies are expected to have formed at the high peaks of the matter density field whose gravitational collapse proceeds quite isotropically (Bardeen et al. 1986; Bernardeau 1994), the void filaments identified from the volume-limited sample would fail to capture the unbiased features of the tidal shear field, no matter how straight they are. In other words, to represent the anisotropic nature of the tidal shear field and its effect on the evolution of the filament galaxies in void regions, the void filament must be identified from the unbiased tracers including the dim galaxies (or low-mass halos). That is why we choose to use a magnitude-limited low-z sample instead of a volume limited high-z sample, even though the latter is a homogeneous one.

A magnitude-limited sample of the nearby void filaments whose redshift is low enough to avoid any false signal caused by the Malmquist bias and whose size is large enough to produce a significant signal is found to correspond to the redshift range $0 \le z \le 0.02$. We find a total of 148 void filaments whose relation between $\tilde{S}$ and $|\bar{M}_r|$ is shown in Figure 5. As can be seen, even at this low redshift bin $0 \le z \le 0.02$, the absolute mean values, $|\bar{M}_r|$, of the void filaments still appear to be correlated with their specific sizes $\tilde{S}$. To quantify the correlation between $|\bar{M}_r|$ and $\tilde{S}$ of the 148 void filaments, we calculate the Pearson product moment coefficient, r, as (Wall & Jenkins 2012):

$$r = \frac{\langle \Delta|\bar{M}_r|\, \Delta\tilde{S}\rangle}{\left[\langle(\Delta|\bar{M}_r|)^2\rangle\langle(\Delta\tilde{S})^2\rangle\right]^{1/2}}\,, \tag{1}$$

where $\Delta|\bar{M}_r| \equiv |\bar{M}_r| - \langle|\bar{M}_r|\rangle$ and $\Delta\tilde{S} \equiv \tilde{S} - \langle\tilde{S}\rangle$. Here $\langle|\bar{M}_r|\rangle$ and $\langle\tilde{S}\rangle$ are the ensemble averages of the mean absolute r-band magnitudes and the specific sizes over the 148 void filaments, respectively, and $\langle(\Delta|\bar{M}_r|)^2\rangle$ and $\langle(\Delta\tilde{S})^2\rangle$ are the corresponding rms fluctuations, respectively.

From the 148 void filaments with four or more member galaxies located at $0 \le z \le 0.02$, we find $r = 0.37 \pm 0.07$ where the errors associated with the estimate of r is also calculated as (Wall & Jenkins 2012)

$$\sigma_r = \frac{1-r^2}{(N_{\rm fil}-1)^{1/2}}\,, \tag{2}$$

where $N_{\rm fil}$ is the number of the void filaments. To see at what confidence level the null hypothesis of no correlation between $|\bar{M}_r|$ and $\tilde{S}$ is rejected, we perform the student-t statistics

as (Wall & Jenkins 2012)

$$t = \frac{r(N_{\rm fil}-2)^{1/2}}{(1-r^2)^{1/2}}\,, \tag{3}$$

where $N_{\rm fil}-2$ is the degree of freedom of the t-variable. Plugging $r=0.37$ and $N_{\rm fil}=148$ into Equation (3), we find that the null hypothesis is rejected at 99.999% confidence level.

Now that we find an observational evidence for the correlation between $\tilde{S}$ and $|\bar{M}_r|$, we would like to investigate if the strength of correlation depends on the richness of the void filaments (i.e., the number of nodes, $N_{\rm node}$). Dividing the void filaments at $0\le z\le 0.02$ into three $N_{\rm node}$-bins, we calculate r separately by using only those void filaments belonging to each $N_{\rm node}$-bin. Figure 6 shows the $\tilde{S}$-$|\bar{M}_r|$ scatter plots for three different bins of $N_{\rm node}$. Table 1 also lists the mean redshifts, the numbers of the void filaments and the estimated values of the Pearson product moment correlation coefficient r between $\tilde{S}$ and $|\bar{M}_r|$ (the fourth column) for three $N_{\rm node}$-bins. As can be read, the richer filaments exhibit stronger correlations between $|\bar{M}_r|$ and $\tilde{S}$. The value of r reaches as high as 0.6 for the richest case of $11\le N_{\rm node}\le 27$. It is also worth noting that the increase of r with $N_{\rm node}$ is not caused by the redshift-difference among the three $N_{\rm node}$-bins.

We have so far followed the frequentist's approach to quantify the correlations between $|\bar{M}_r|$ and $\tilde{S}$. However, the reliability of the frequentist's approach depends on the sample size. Given that the numbers of the low-z void filaments at each $N_{\rm node}$-bin are not large enough to guarantee the success of the frequentist's approach, we also take the Bayesian approach by computing the posterior probability density distribution of the true correlation coefficient, ρ as (Wall & Jenkins 2012)

$$p(\rho|r,{\rm data}) \propto \frac{(1-\rho^2)^{\frac{N_{\rm fil}-1}{2}}}{(1-r\rho)^{N_{\rm fil}-\frac{3}{2}}}\left[1+\frac{1}{N_{\rm fil}-\frac{1}{2}}\frac{1+r\rho}{8}+\cdots\right]\,, \tag{4}$$

where $p(\rho|r,{\rm data})$ represents the conditional probability of ρ provided that the Pearson product moment correlation coefficient has the value of r at each $N_{\rm node}$-bin. Here, we assume a flat prior for $p(r)$ and normalized $p(\rho|r,{\rm data})$ to satisfy $\int p(\rho|r,{\rm data})=1$. The left, middle and right panels of Figure 7 show $p(\rho|r,{\rm data})$, for the cases of $4\le N_{\rm node}\le 6$, $7\le N_{\rm node}\le 10$ and $11\le N_{\rm node}\le 27$, respectively. As can be seen, the maximum probability is achieved when the true correlation coefficient exceeds 0.6 for the case of the richest filaments, supporting the results obtained from the frequentist's approach.

The observed trend that the correlation between $|\bar{M}_r|$ and $\tilde{S}$ becomes stronger with the richness of the void filament can be understood as follows. The richer void filaments correspond to deeper gravitational potential well which can accommodate larger amounts of cold gas, which in turn can be transported even to the central regions of the voids from the

surroundings if the void filaments are more spatially extended. In consequence, the mean luminosity of the void galaxies located in the richer filaments would develop more sensitive dependence on the spatial extents of the filamentary networking.

It may be worth examining the dependence of the final result on how to quantify the degree of the straightness of the void filaments. As in the original work of Park & Lee (2009b), we measure the linearity $R_{\rm L}$ of the 148 void filaments and investigate the correlations between $R_{\rm L}$ and $|\bar{M}_r|$ at three $N_{\rm node}$-bins, which are shown in Figure 8. The Pearson product moment correlation coefficients between $R_{\rm L}$ and $|\bar{M}_r|$ for the three different $N_{\rm node}$-bin are listed in the fifth column of Table 1. As can be seen, no correlation is found between $R_{\rm L}$ and $|\bar{M}_r|$, which is inconsistent with the result of Park & Lee (2009b) whose numerical analysis found the existence of a strong correlation $r = 0.67$ between them. To understand where this inconsistency stems from, we examine how strongly $R_{\rm L}$ and $\tilde{S}$ are correlated with each other for the three $N_{\rm node}$-bins, the results of which are shown in Figure 9 and listed in the sixth column of Table 1 . As can be seen, a signal of mild correlation is found for the case of $7 \le N_{\rm node} \le 11$ but no signal at all for the other two cases.

Note that for the case of $4 \le N_{\rm node} \le 6$, the linearity tends to be biased toward high values of $0.4 \le R_{\rm L} \le 1$. As explained in Park & Lee (2009b), for the case that the filaments have small number of nodes, the linearity $R_{\rm L}$ is prone to high values, failing to represent well the degree of filament straightness. For the case of the rich filaments with large number of nodes, the linearity $R_{\rm L}$ is a good indicator of the filament straightness only provided that the positions of the nodes are measured with high accuracy. When the measurements are done in the redshift space, however, the redshift-space errors would contaminate the measurement of each of the positions of the nodes, which would propagate into the errors in the measurements of the total lengths of the filaments. The larger numbers of the nodes a filament has, the larger amount of propagated error would contaminate the measurement of its total length which would in turn cause large uncertainties in the estimate of its linearity.

4. SUMMARY AND DISCUSSION

The aim of this work was to observationally test the scenario suggested by Park & Lee (2009b) that the void galaxies located in the more straight filaments would be more luminous since the efficacy of the gas accretion along the void filaments into the void galaxies increases with the degree of the straightness of the void filaments. The catalog of the giant galaxy voids constructed by Pan et al. (2012) from the SDSS DR7 datasets with the help of the HV02 void finding algorithm (Hoyle & Vogeley 2002) has been used as the parent sample and the MST-based filament finder was employed to identify the filamentary structures in

the galaxy voids.

Determining the specific size (size per node, $\tilde{S}$) of each void filament as a measure of its straightness and the mean absolute value of the absolute r-band magnitude $|\bar{M}_r|$ of the member galaxies, we investigated if and how $|\bar{M}_r|$ is correlated with $\tilde{S}$ on average by measuring the Pearson product moment correlation coefficient, r, between the two quantities. To avoid a false signal of correlation between $\tilde{S}$ and $|\bar{M}_r|$ caused by the Malmquist bias, we have focused only on the lowest redshift for the detection of the bridge effect. From a total of 148 void filaments consisting of four or more member galaxies (nodes) in the redshift range of $0 \le z \le 0.02$, it is found to be $r = 0.37 \pm 0.07$. Although this observational signal is not quantitatively consistent with the numerical estimate, $r = 0.67$, by Park & Lee (2009b) based on the Millennium run semi-analytic galaxy catalog (Springel et al. 2005), it is a five sigma signal and thus may be regarded as the observational evidence for the existence of the bridge effect of the void filaments.

We have also inspected if and how the strength of correlation between $|\bar{M}_r|$ and $\tilde{S}$ changes with the node number $N_{\rm node}$ of the void filaments (i.e., the *richness* of the void filaments) and noted a trend that the value r gradually increases with the richness of the void filament. Our explanation for this trend is as follows. A richer filament must correspond to a deeper well of the gravitational potential that could accommodate larger amounts of gas inflow from the surroundings. In consequence the void galaxies located in a richer filament would develop more sensitive dependence on the degree of the straightness of void filament.

The straightness of the void filaments reflects how anisotropic the spatial distributions of the void galaxies are. As the voids evolve and their densities decrease, they would become more susceptible to the external tidal forces, which in turn augment the degree of the anisotropy of the spatial distributions of the void galaxies. In other words, the capacity of the void filaments as a transportation channel would increase in the nonlinear stage of the void evolution where the tidal shear field develop nonlinear correlations. In consequence, the star formation activity in the void galaxies would become stimulated by the efficient supply of the cold gases along the straight void filaments. The presence of the bridge effect of void filaments that has been confirmed by our observational analysis may provide an important clue to the mechanism through which the void galaxies become gas richer, bluer colored, and have higher specific star formation rates than their wall counterparts (e.g., Rojas et al. 2004; Kreckel et al. 2011; Beygu et al. 2013; Ricciardelli et al. 2014).

However, we have yet to answer the fundamental question of what caused the bridge effect of void filaments. A more comprehensive study based on cosmological hydrodynamic simulations will be desirable to quantitatively understand why and how the accretion of cold gas occur more efficiently along the straight filaments that emerge during the nonlinear

stage of the void evolutions. Also, in the original work of Park & Lee (2009b), not only the mean luminosity but also the mean mass of the central blackholes of the void galaxies were found to be higher in the more straight void filaments. In fact, it was the mean mass of the central blackholes that yielded the strongest correlation with the degree of the straightness of the void filaments. Although it is very hard to measure directly the masses of the central blackholes, the X-ray luminosities of the void galaxies with active galactic nuclei (AGN), if any, could be used to quantify how massive their central blackholes are. Our future work will focus on searching for the AGN galaxies in the void regions and exploring observationally if and how their AGN activities are correlated with the degree of the straightness of the void filaments.

We thank a referee for his/her very enlightening comments on the Malmquist bias. JS was financially supported by the Basic Science Research Program through the National Research Foundation of Korea (NRF) funded by the Ministry of Education (NRF-2014H1A8A1022479). JL was financially supported by the Basic Science Research Program through the NRF funded by the Ministry of Education (NO. 2013004372) and by the research grant from the NRF to the Center for Galaxy Evolution Research (NO. 2010-0027910). FH acknowledges support from Pontifica Universidad Catolica del Ecuador.

REFERENCES

Abazajian, K. N., Adelman-McCarthy, J. K., Agüeros, M. A., et al. 2009, ApJS, 182, 543

Alpaslan, M., Robotham, A. S. G., Obreschkow, D., et al. 2014, MNRAS, 440, L106

Aragon-Calvo, M. A., & Szalay, A. S. 2013, MNRAS, 428, 3409

Bardeen, J. M., Bond, J. R., Kaiser, N., & Szalay, A. S. 1986, ApJ, 304, 15

Barrow, J. D., Bhavsar, S. P., & Sonoda, D. H. 1985, MNRAS, 216, 17

Bernardeau, F. 1994, ApJ, 427, 51

Beygu, B., Kreckel, K., van de Weygaert, R., van der Hulst, J. M., & van Gorkom, J. H. 2013, AJ, 145, 120

Bond, J. R., Kofman, L., & Pogosyan, D. 1996, Nature, 380, 603

Colberg, J. M. 2007, MNRAS, 375, 337

El-Ad, H., & Piran, T. 1997, ApJ, 491, 421

Gottlöber, S., Łokas, E. L., Klypin, A., & Hoffman, Y. 2003, MNRAS, 344, 715

Hoyle, F., & Vogeley, M. S. 2002, ApJ, 566, 641

Kreckel, K., Platen, E., Aragón-Calvo, M. A., et al. 2011, AJ, 141, 4

Kreckel, K., Croxall, K., Groves, B., van de Weygaert, R., & Pogge, R. W. 2015, ApJ, 798, LL15

Malmquist, K. G. 1936, Stockholms Observatoriums Annaler, 12, 7

Pan, D. C., Vogeley, M. S., Hoyle, F., Choi, Y.-Y., & Park, C. 2012, MNRAS, 421, 926

Park, D., & Lee, J. 2009a, MNRAS, 397, 2163

Park, D., & Lee, J. 2009b, MNRAS, 400, 1105

Patiri, S. G., Prada, F., Holtzman, J., Klypin, A., & Betancort-Rijo, J. 2006, MNRAS, 372, 1710

Rieder, S., van de Weygaert, R., Cautun, M., Beygu, B., & Portegies Zwart, S. 2013, MNRAS, 435, 222

Ricciardelli, E., Cava, A., Varela, J., & Quilis, V. 2014, MNRAS, 445, 4045

Rojas, R. R., Vogeley, M. S., Hoyle, F., & Brinkmann, J. 2004, ApJ, 617, 50

Sahni, V., Sathyaprakah, B. S., & Shandarin, S. F. 1994, ApJ, 431, 20

Shim, J., & Lee, J. 2013, ApJ, 777, 74

Springel, V., White, S. D. M., Jenkins, A., et al. 2005, Nature, 435, 629

van de Weygaert, R., & van Kampen, E. 1993, MNRAS, 263, 481

van de Weygaert, R., & Bond, J. R. 2008, A Pan-Chromatic View of Clusters of Galaxies and the Large-Scale Structure, 740, 335

Wall, J. V., & Jenkins, C. R. 2012, Practical Statistics for Astronomers, (Cambridge, UK: Cambridge University Press)

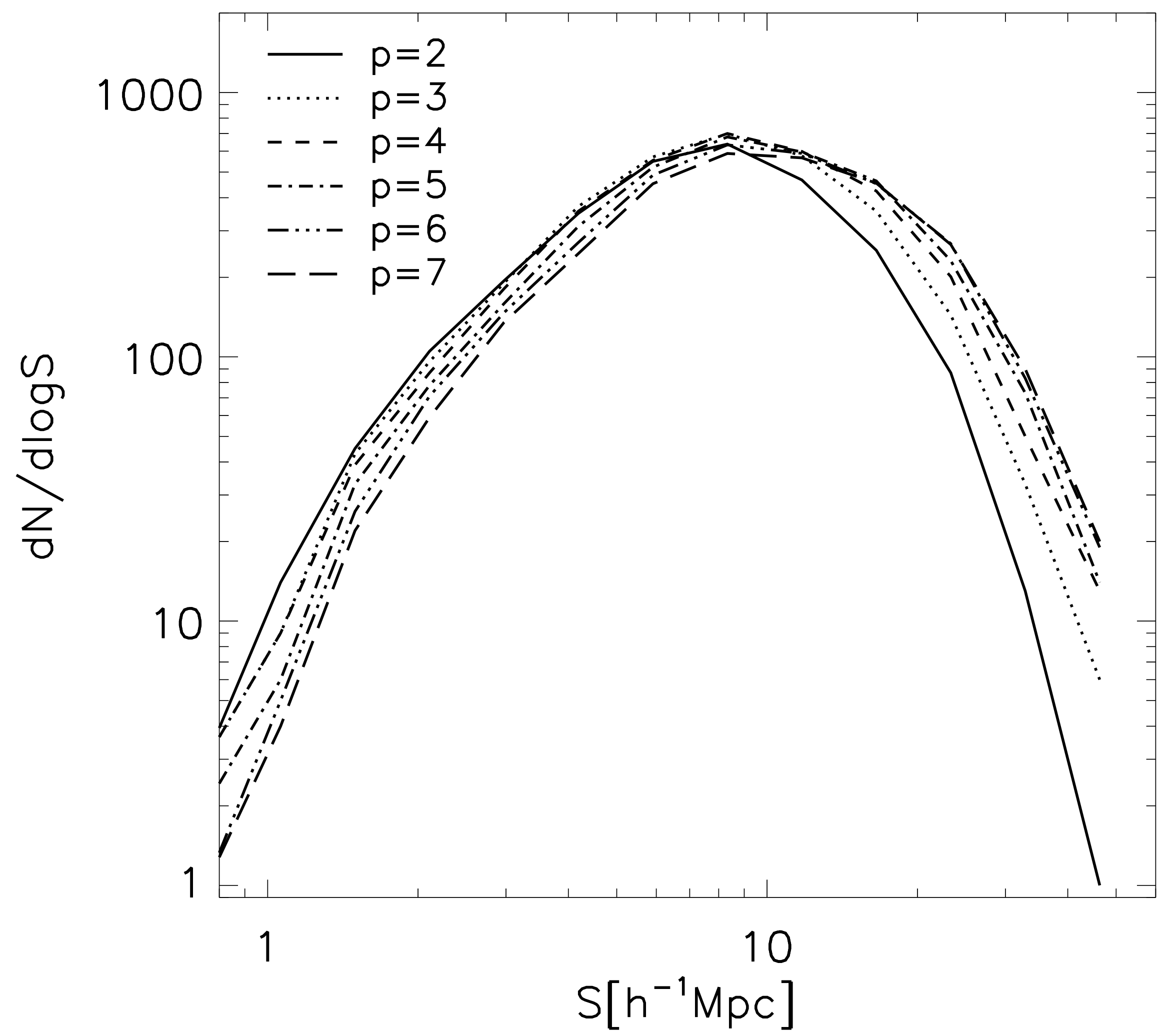

Fig. 1.— Size distribution of the void mini-filaments for six different cases of the pruning level p. Here, a void filament represents the primary structure of a MST from which the minor twigs having less than p nodes are removed and its size S is define as its spatial extent. It is clear that the convergence of $dN/d\log S$ in the large S-section appears at $p \geq 5$.

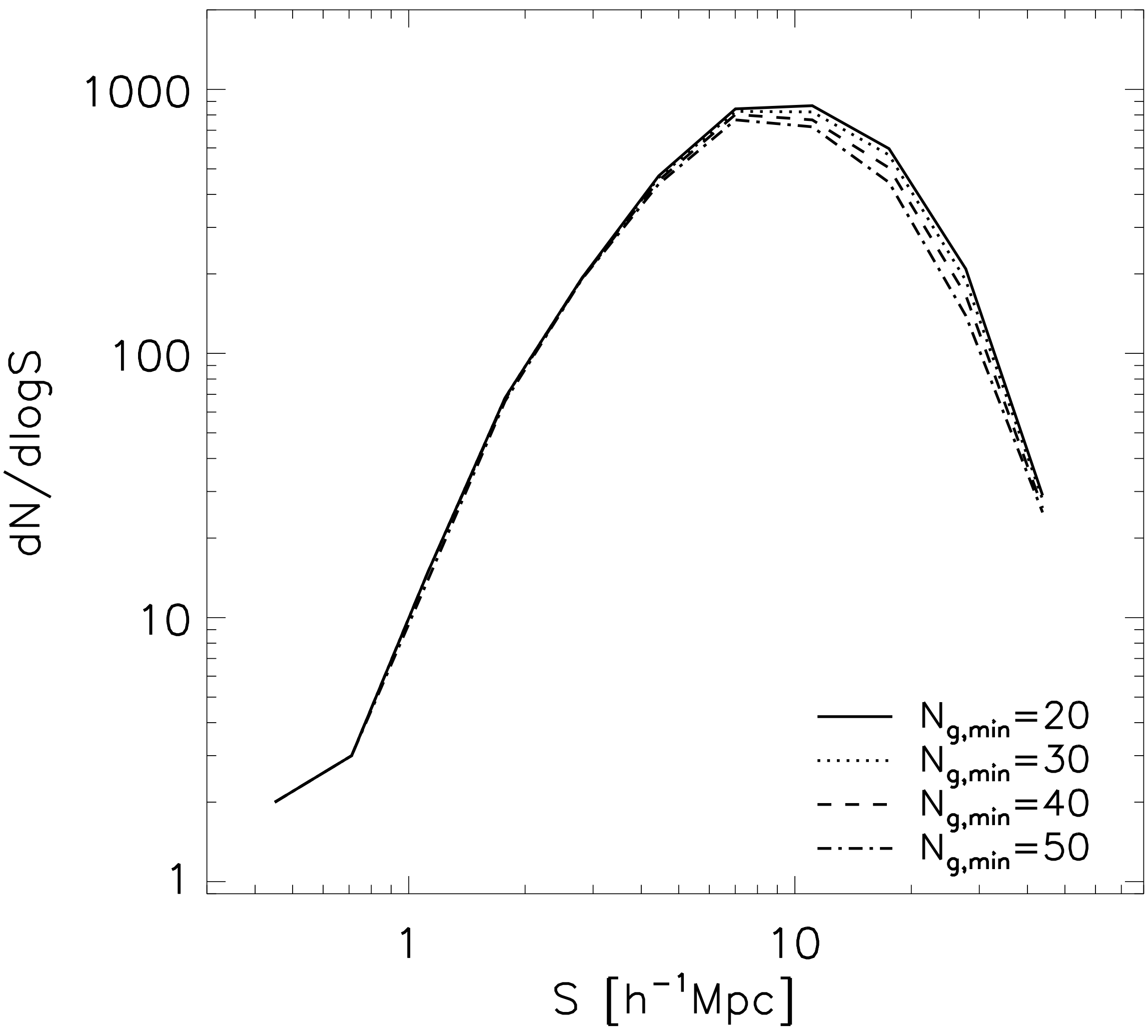

Fig. 2.— Number distribution of the sizes of void filaments in interval $[\log S, \log S + d\log S]$ for four various minimum number of galaxies in a void $N_{g,min}$ applied for the giant void selection.

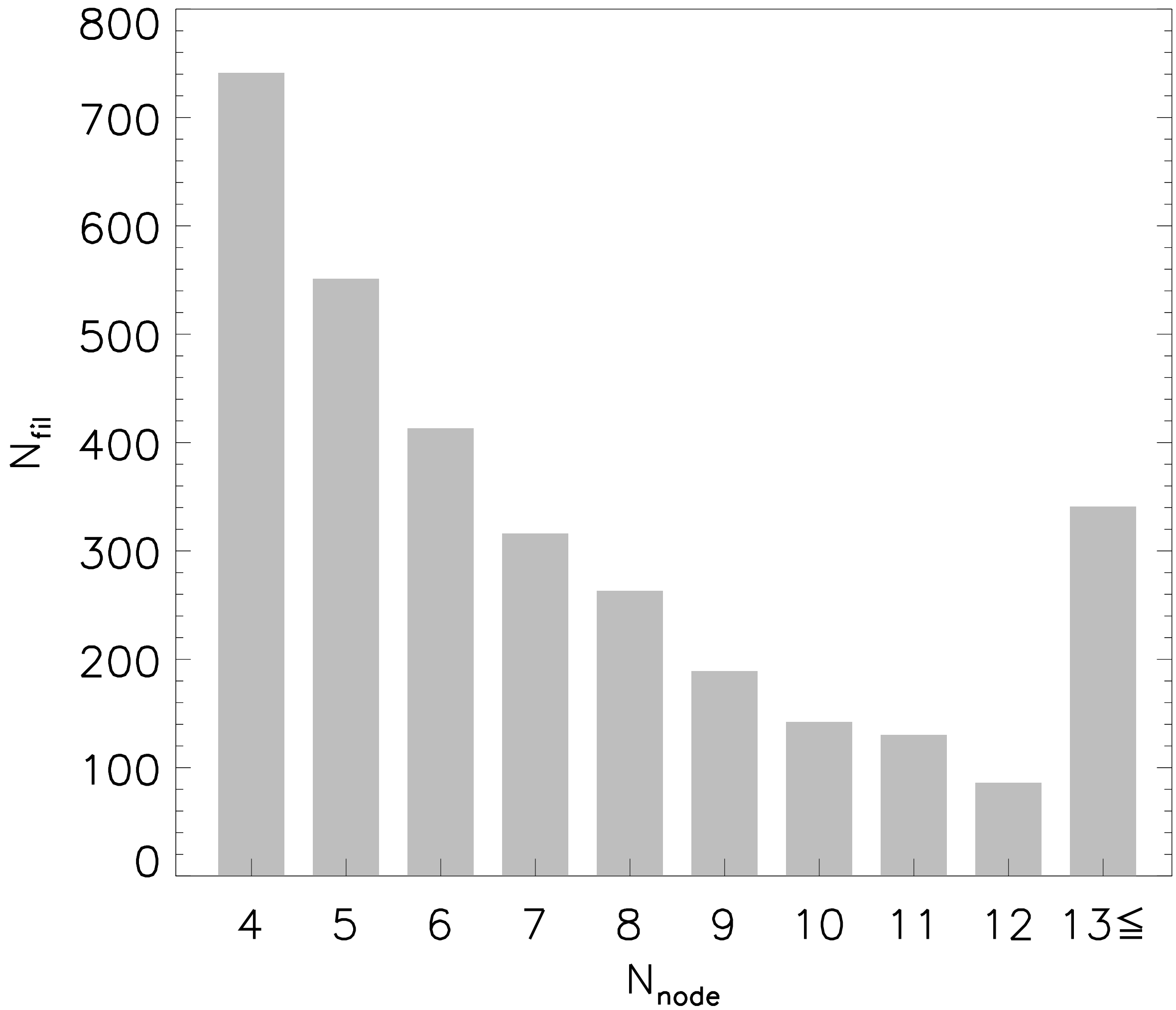

Fig. 3.— Number counts of the void filaments having four or more nodes from the Sloan void catalog by Pan et al. (2012) as a function of the node number, $N_{\rm node}$.

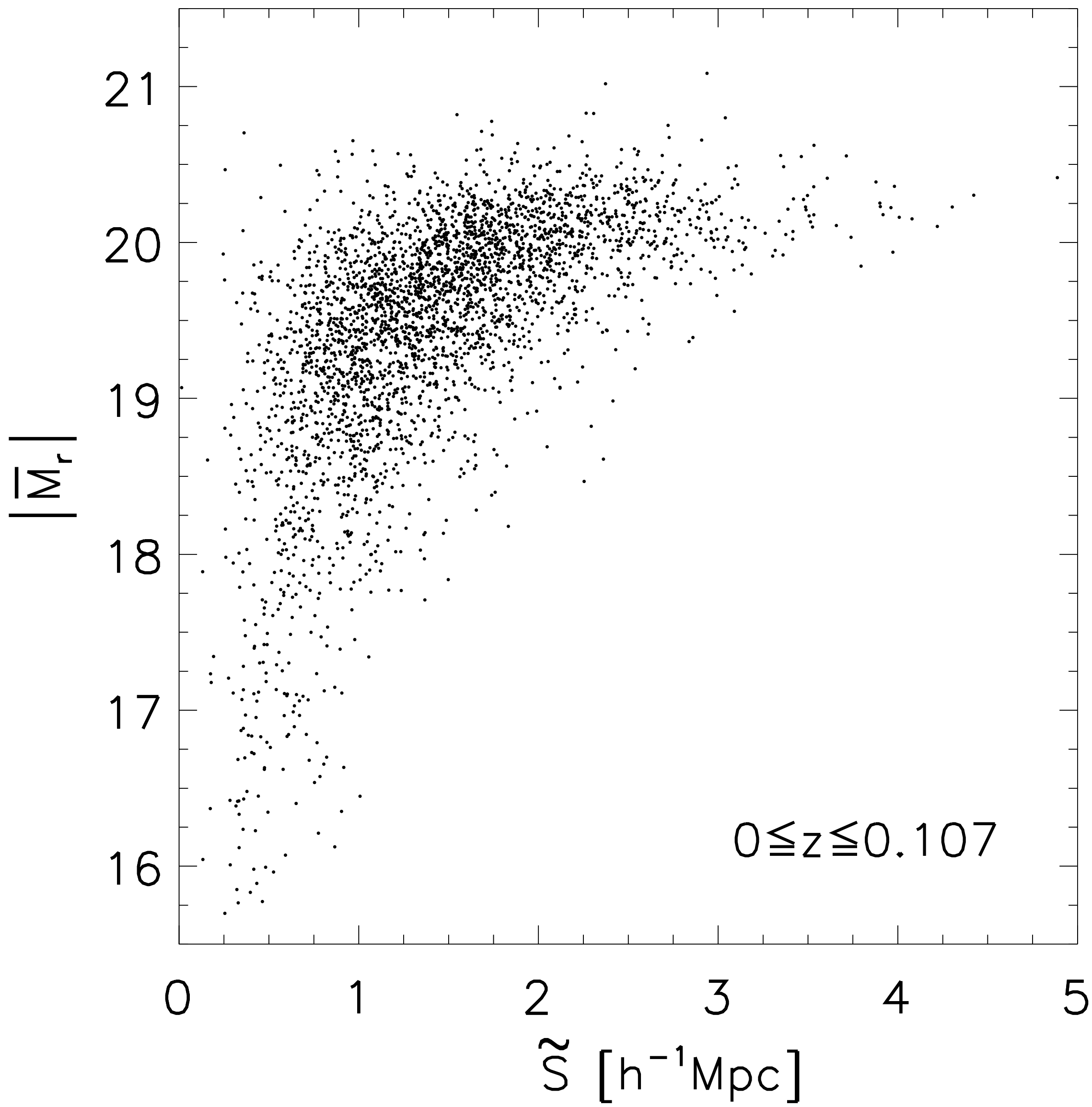

Fig. 4.— Specific sizes of the 3172 void filament $\tilde{S} \equiv S/N_{\rm node}$ (size per node) versus the mean absolute r-band magnitude of its member galaxies $|\bar{M}_r|$ from our sample.

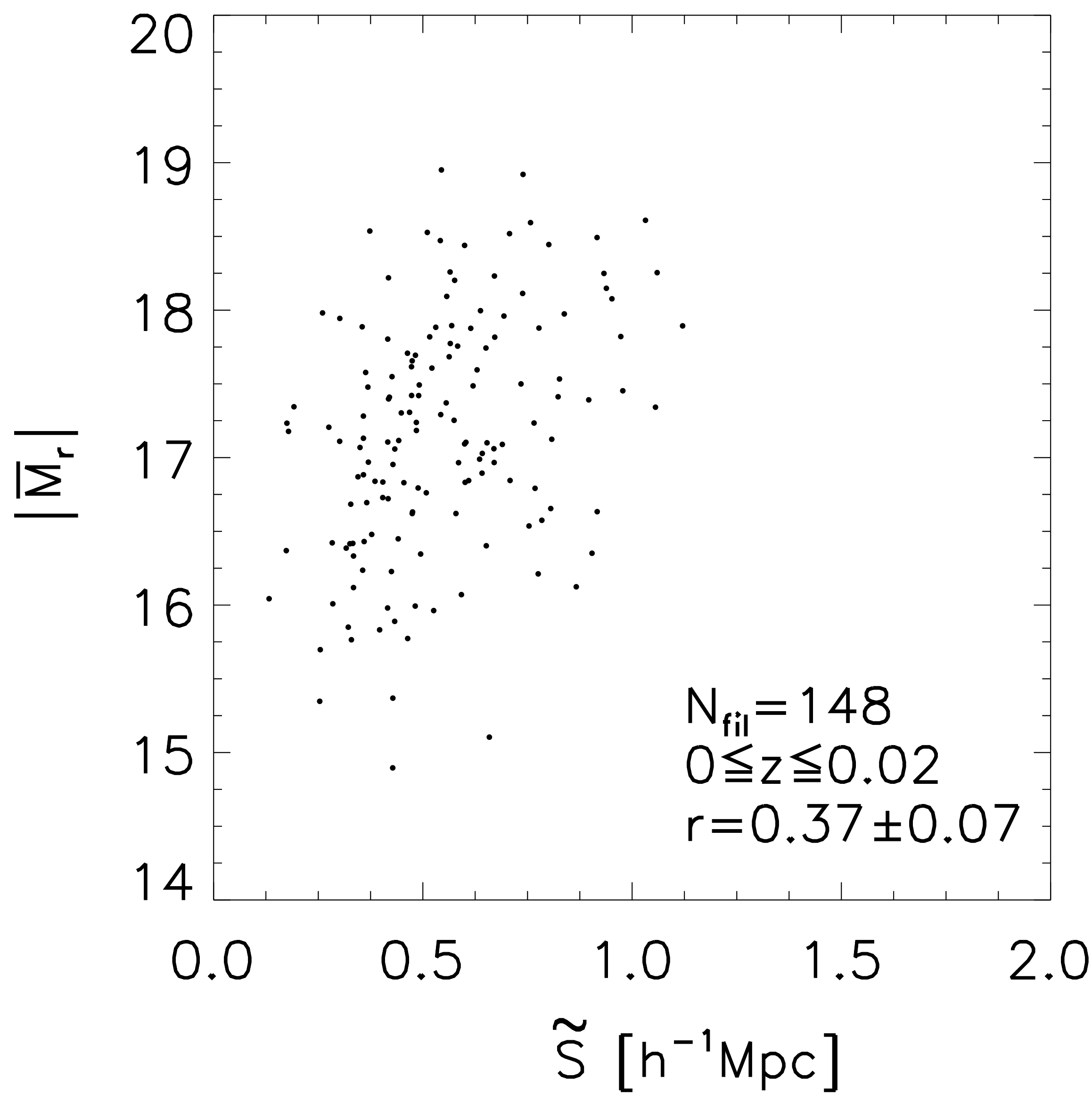

Fig. 5.— A total of 148 void filaments with four or more member galaxies at $0 \leq z \leq 0.02$ from the Sloan void catalog of Pan et al. (2012) in the $\tilde{S} - |\bar{M}_r|$ plane.

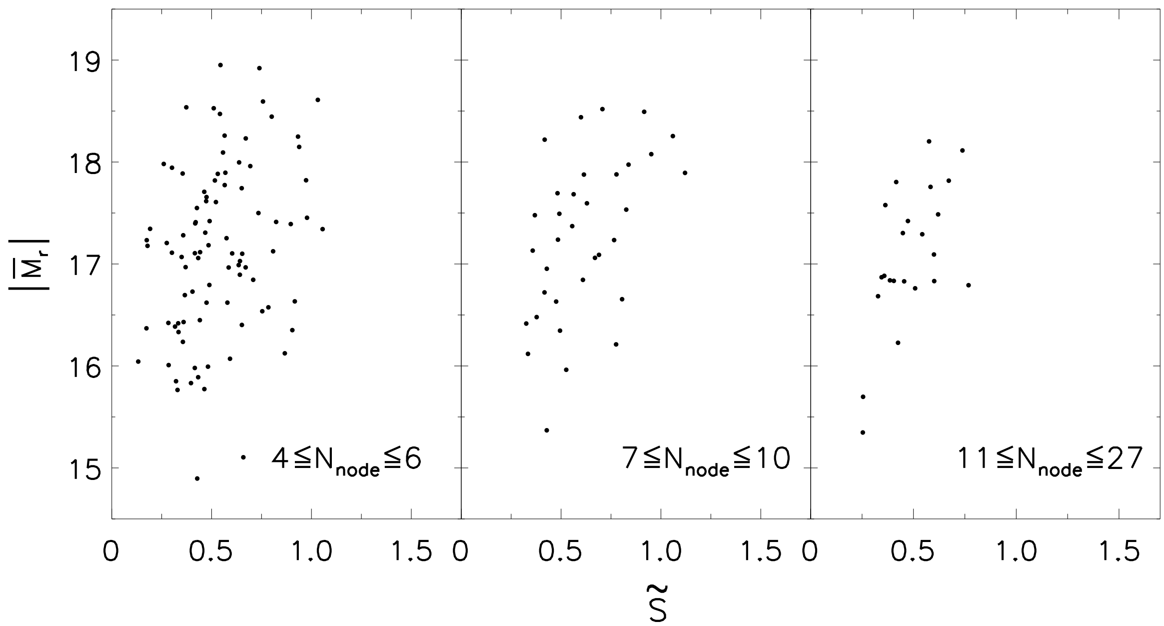

Fig. 6.— Same as Figure 5 but for three different bins of the node number $N_{\rm node}$.

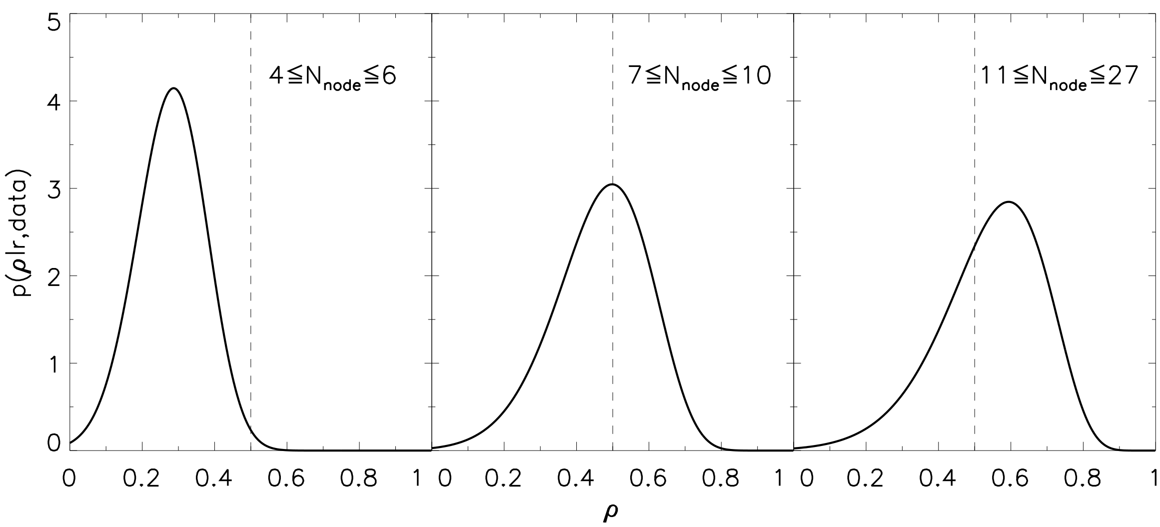

Fig. 7.— Posterior probability density distribution of the real correlation coefficient ρ provided that the Pearson product moment correlation coefficient r has the resulting value from our sample at $0 \leq z \leq 0.02$ for three different cases of $N_{\rm node}$ (solid line). In each panel the dashed line corresponds to the case of a mild correlation ($\rho = 0.5$).

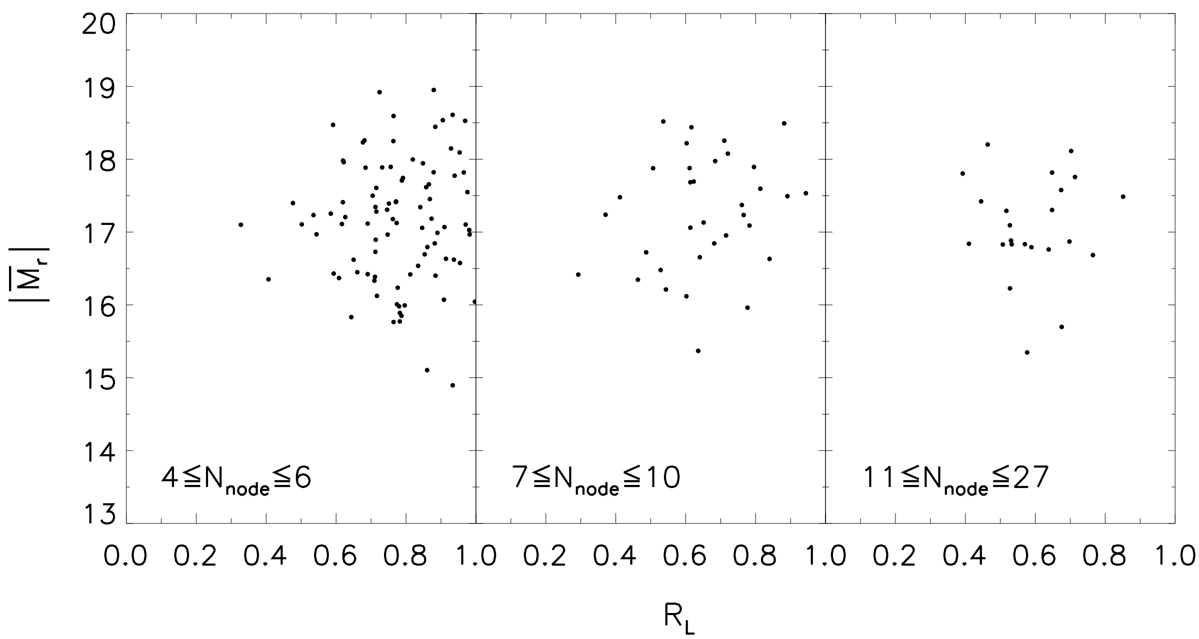

Fig. 8.— Same as Figure 6 but replacing the specific size $\tilde{S}$ by the linearity $R_{\rm L}$ to represent the degree of the straightness of the void filaments.

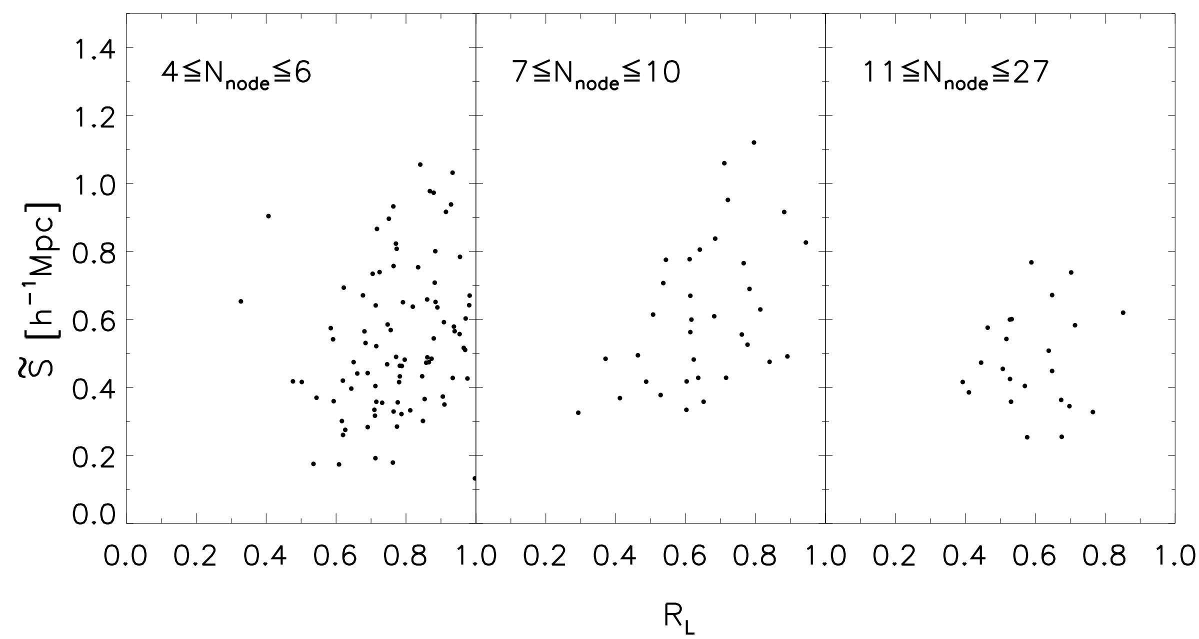

Fig. 9.— Specific sizes $\tilde{S}$ of 148 void filaments versus their linearities R_{L}.

Table 1. Richness ($N_{\rm node}$), mean redshift ($\bar{z}$), number of the void filaments ($N_{\rm fil}$) and Pearson product moment correlation coefficients (r).

$N_{\rm node}$	$\bar{z}$	$N_{\rm fil}$	$\mathrm{r}(\tilde{S}, \lvert\bar{M}_r\rvert)$	$\mathrm{r}(R_L, \lvert\bar{M}_r\rvert)$	$\mathrm{r}(R_L, \tilde{S})$
[4, 6]	0.012 ± 0.005	91	0.29 ± 0.10	0.04 ± 0.10	0.21 ± 0.10
[7, 10]	0.014 ± 0.003	34	0.50 ± 0.13	0.21 ± 0.16	0.46 ± 0.14
[11, 27]	0.013 ± 0.004	23	0.60 ± 0.13	0.00 ± 0.21	0.10 ± 0.21